

Modeling and simulation technique of brushless DC motor for phase control by operation mode

Young-Sun Kim

Professor, Department of Electrical and Electronic Engineering, Joongbu University, Goyang, 10279, Korea
yskim@joongbu.ac.kr

Abstract

BLDC motors offer several advantages over brushed DC motors, including phase angle control of an applied AC source, more torque per weight, more torque per watt, increased reliability, reduced noise, longer lifetime, elimination of commutation sparks from the commutator, and overall reduction of electric and magnetic interference. A brushless direct current motor (BLDCM) has rotating permanent magnets and a fixed armature, eliminating problems associated with supplying current to the moving armature. An electronic switching controller replaces the brush and commutator assembly of the BLDCM, which continually switches the phase to the armature windings to keep the motor operating. This work represents a modeling scheme to analyze the characteristic of the BLDC motor according to variation of firing angle. A cutset equation was established for each switching mode and a system graph was presented. In addition, a state equation expressed as a differential equation for the switching mode was established and analyzed by the Runge-Kutta method. In this paper, the rotation speed of the brushless DC motor is assumed to be constant, and the counter electromotive force of the stator winding is assumed to be a sinusoidal wave. Also, a line current, phase current of the winding and developed torque are calculated and harmonic analysis for winding current is performed according to various firing angle of applied source. In the future, verification through comparison of numerical analysis results with experimental results is required.

Keywords: Brushless dc motor, Firing angle, Harmonic analysis, Phase angle control, Torque.

1. Introduction

AC motors used for control in industrial sites can be classified into induction type and synchronous type. Among them, the synchronous type motors used for small and medium capacity have the control performance of DC motors and the robustness of AC motors. There are two types of permanent magnet type synchronous motors that include a permanent

magnet in the rotor, whose back electromotive force is a sine wave and a trapezoid. The latter of these is called a brushless DC motor [1,2]. DC motors are widely used because they have relatively high efficiency compared to small size and have properties suitable for speed and position control [3]. However, the only drawback is that it has mechanical switches called brushes and commutators. Since the brush is moving the commutator at high speed, graphite or metal powder is scattered around the abrasion of the brush and commutator segments [4]. In addition, it is environmentally vulnerable due to the problem of sparks occurring between the brush and the commutator [5].

The BLDC motor is designed to increase durability and suitable for high-speed rotation by removing the brush part inside the general DC motor. In addition, it does not increase noise or degrade performance even when used for a long time compared to general motors, and it is economical due to its precise speed control and high energy efficiency [6,7]. AC motors have long durability and high noise and power consumption. DC motors have short durability, but low power consumption and high noise. The BLDC motor, which complements the characteristics of the two motors, is semi-permanent in terms of durability, produces low noise, and consumes very little power. AC motors can only operate in one direction, whereas DC motors and BLDC motors have the characteristic of being able to operate in both directions. As such, compared to AC motors, Also, BLDC motors have the advantages of low noise, accurate control, low heat generation and high durability [8,9]. BLDCM is a type of synchronous motor that applies AC voltage to the three-phase stator winding by switching the inverter to the DC voltage by the position detector. However, unlike general synchronous motors, BLDCM uses an AC voltage generated by an inverter as a power source, so the power source contains many harmonics. On the other hand, it has the advantage of controlling the phase angle of the applied AC voltage by adjusting the switching timing of the inverter [10].

In this study, a switching mode instead of a commutator using six inverters to drive a BLDC motor was presented. A cutset equation was established for each switching mode and a system graph was presented. In addition, a state equation expressed as a differential equation for the switching mode was established and analyzed by the Runge-Kutta method. As

a result the harmonic current and torque characteristics according to the phase angle control were analyzed for each of the stator windings (armature windings) of a BLDC motor in delta(Δ) connection.

2. Characteristic Equations according to Operation Mode

In this chapter, the driving of the motor by the inverter is explained and the state equation for a specific mode is derived. In addition, the current relational expression according to the switching mode and simulation flow chart are presented.

2.1. Analysis modeling

A three-phase bridge type BLDC motor has the same

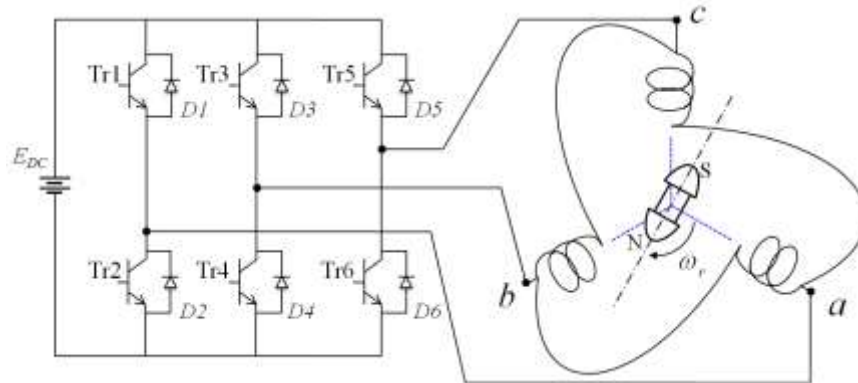


Figure 1. Two pole three phase brushless DC motor driving circuit

The winding of the stator can be either Δ connection or Y connection, so in this study, a brushless DC motor was modeled mathematically for each case of Δ connection. In addition, it is intended to analyze the variation characteristics

of the harmonic current component and generated torque according to the phase angle control. The order of switching varies depending on the purpose of the motor, but the most basic truth table is shown in Table 1.

Table 1: Truth table for inverter

Mode	Tr.	I	II	III	IV	V	VI	I
SW Open/Close 1 : ON 0 : OFF	Tr1	1	1	0	0	0	1	1
	Tr2	0	0	1	1	1	0	0
	Tr3	0	1	1	1	0	0	0
	Tr4	1	0	0	0	1	1	1
	Tr5	0	0	0	1	1	1	0
	Tr6	1	1	1	0	0	0	1
Potential at U, V, W	U	E	E	0	0	0	E	E
	V	0	E	E	E	0	0	0
	W	0	0	0	E	E	E	0
Terminal voltage	U-V	E	0	-E	-E	0	E	E
	V-W	0	E	E	0	-E	E	0
	W-U	-E	-E	0	E	E	0	-E

Figure 2 is the circuit shown to explain the overall operation of the operation characteristics of the 2-pole 3-phase BLDCM. It shows that a switch and a unidirectional diode are used to carry out current, just as a brush and a commutator perform a commutation operation in a DC motor. According to the truth table in Table 1, even if the switching for each mode is changed, the mechanism by which the flow of current in the BLDCM is changed through these repeated operations can be known.

As shown in Figure 2, in BLDCM, the reference position of the permanent magnet rotor is the position where the largest

induced voltage is generated in the u-coil, that is, the position where the permanent magnet rotor is placed in a direction perpendicular to the u-coil as the reference position. When the reference position is set in this way, the induced voltage equation is as shown in (1).

$$\begin{aligned}
 e_u &= K_\omega \sin(\theta + \pi/2 - \theta_0) \\
 e_v &= K_\omega \sin(\theta + \pi/2 - \theta_0 - 2\pi/3) \\
 e_w &= K_\omega \sin(\theta + \pi/2 - \theta_0 + 2\pi/3)
 \end{aligned}
 \tag{1}$$

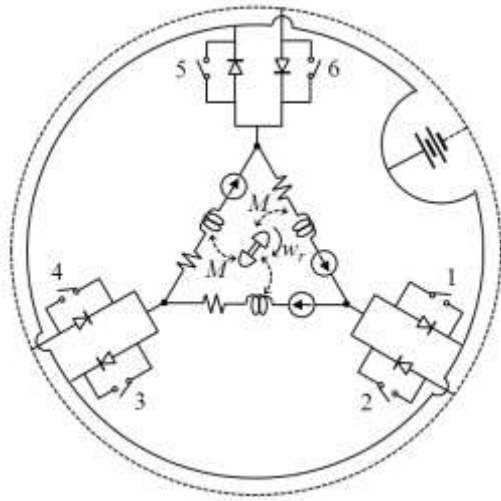
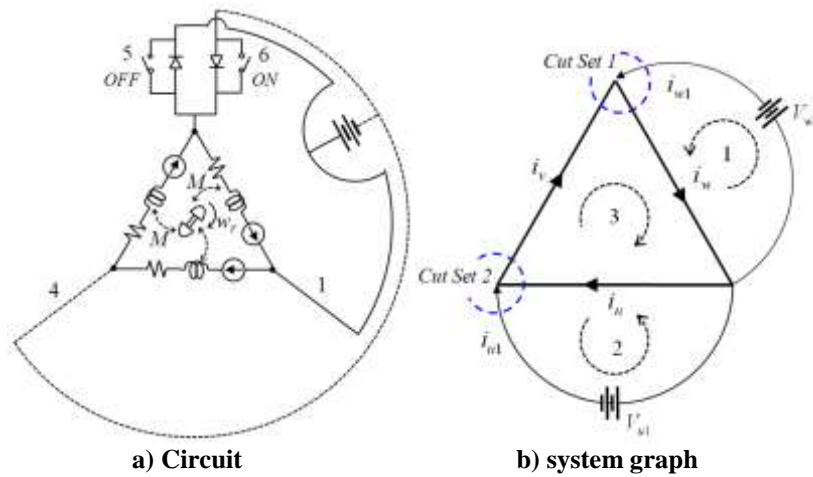


Figure 2. Operating characteristics circuit diagram of BLDCM

2.2 Analysis system for switching mode I

As shown in the truth table, the first interpretation mode is the moment from mode VI to mode I, and Tr1, Tr4, and Tr5 are in the ON state. Then, Tr5 is turned off and Tr6 is turned on. Figure 3 shows the operating circuit and system graph in mode I.



a) Circuit
b) system graph
Figure 3. Operating circuit and system diagram

The terminal voltage equation in mode I is expressed as (2).

$$\begin{Bmatrix} V_u \\ V_v \\ V_w \end{Bmatrix} = \begin{bmatrix} R + Lp & -M p & -M p \\ -M p & R + Lp & -M p \\ -M p & -M p & R + Lp \end{bmatrix} \begin{Bmatrix} i_u \\ i_v \\ i_w \end{Bmatrix} + \begin{Bmatrix} e_u \\ e_v \\ e_w \end{Bmatrix} \quad (2)$$

Here, p is a differential operator and means d/dt . When KVL(Kirchhoff's Voltage Law) is applied to the three closed loops in the system graph of Figure 3(b), it is as shown in (3).

$$\begin{aligned} -V_{w1} + V_w &= 0 \\ V_{u1} + V_u &= 0 \\ V_{u1} - V_{w1} + V_v &= 0 \end{aligned} \quad (3)$$

$$\begin{bmatrix} -1 & 0 & 1 & 0 & 0 \\ 1 & -1 & 0 & 1 & 0 \\ 1 & 0 & 0 & 0 & 1 \end{bmatrix} \begin{Bmatrix} V_{u1} \\ V_{w1} \\ V_u \\ V_v \\ V_w \end{Bmatrix} = 0 \quad (4)$$

A cutset matrix is a minimum equation set of branches of a connected graph such that the removal of these branches causes the graph to be cut into exactly two parts. If a closed surface is taken for any node, the algebraic sum of currents

flowing in and out through this closed surface is zero. This is the same as KCL(Kirchhoff's Current Law) and is called the cutset equation.

$$\begin{aligned} i_{u1} + i_u - i_v &= 0 \\ i_{w1} + i_v - i_w &= 0 \end{aligned} \quad (5)$$

If the above cutset equation is expressed in matrix form, it is as shown in (6).

$$\begin{bmatrix} 1 & 0 & 1 & -1 & 0 \\ 0 & 1 & 0 & 1 & -1 \end{bmatrix} \begin{Bmatrix} i_{u1} \\ i_{w1} \\ i_u \\ i_v \\ i_w \end{Bmatrix} = 0 \quad (6)$$

Applying KVL and KCL to the cutset circuit to express the terminal voltage equation is as follows.

$$\begin{Bmatrix} V_{u1} \\ 0 \\ -V_{w1} \end{Bmatrix} = \begin{bmatrix} R + Lp & -M p & -M p \\ -M p & R + Lp & -M p \\ -M p & -M p & R + Lp \end{bmatrix} \begin{Bmatrix} i_u \\ i_v \\ i_w \end{Bmatrix} + \begin{Bmatrix} e_u \\ e_v \\ e_w \end{Bmatrix} \quad (7)$$

Since it is in the form of a differential equation of the voltage

equation, it is necessary to slightly change the form of the equation to interpret it. If the inductance and the resistance are separated and the derivative term is transposed to the left side using its inverse matrix, the terminal voltage equation is as shown in (8).

$$p \begin{Bmatrix} i_u \\ i_v \\ i_w \end{Bmatrix} = - \begin{bmatrix} L & -M & -M \\ -M & L & -M \\ -M & -M & L \end{bmatrix}^{-1} \begin{bmatrix} R & 0 & 0 \\ 0 & R & 0 \\ 0 & 0 & R \end{bmatrix} \begin{Bmatrix} i_u \\ i_v \\ i_w \end{Bmatrix} + \begin{bmatrix} L & -M & -M \\ -M & L & -M \\ -M & -M & L \end{bmatrix}^{-1} \left(\begin{Bmatrix} V_{u1} \\ 0 \\ -V_{w1} \end{Bmatrix} - \begin{Bmatrix} e_u \\ e_v \\ e_w \end{Bmatrix} \right) \quad (8)$$

If the stator winding of the motor is Δ connection, the line current of the combination of phase currents can be calculated. The following is the relationship between phase current and line current for mode I.

$$\begin{aligned} i_{ul} &= -i_{u1} + i_{w1} \\ i_{vl} &= -i_{u1} \\ i_{wl} &= -i_{w1} \end{aligned} \quad (9)$$

By constructing the cut-set equation for each mode using the above algorithm, the current characteristics for each phase can be calculated. When BLDCM is driven with square wave voltage, the characteristics of current and back electromotive force also change every 60° . Since the torque occurs in U, V and W phases, the generated torque is as follows.

$$T_e = T_u + T_v + T_w = \frac{(e_u i_u + e_v i_v + e_w i_w)}{\omega_r} \quad (10)$$

2.3 System graph and current definition for other switching sequences(mode II – VI)

Depending on the switching sequence, the ON and OFF of Transistor can be determined and an equation can be established at each cutset. Also, by substituting this cut-set equation into the terminal voltage equation, a differential equation can be established that can calculate the characteristics of each mode. Figure 4 is a system graph

according to mode and shows the cutset location and circuit diagram.

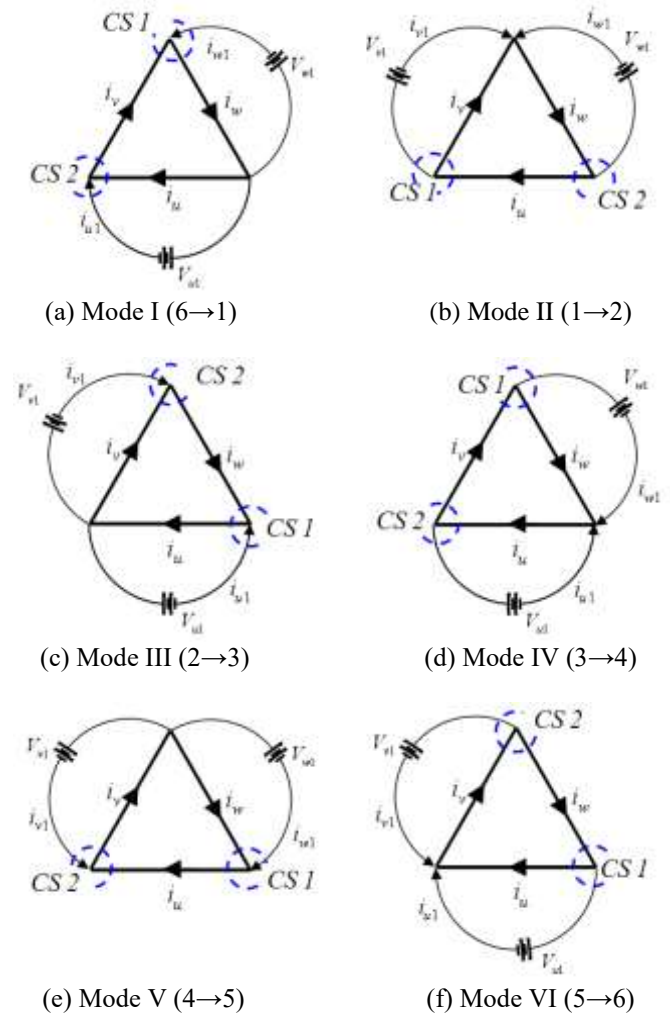


Figure 4. System diagrams according to operation mode

Table 2: Line current expression according switching mode

Mode I	Mode II	Mode III
$i_{ul} = -i_{u1} + i_{w1}$ $i_{vl} = -i_{u1}$ $i_{wl} = -i_{w1}$	$i_{ul} = i_{w1}$ $i_{vl} = i_{v1}$ $i_{wl} = -i_{v1} - i_{w1}$	$i_{ul} = -i_u$ $i_{vl} = i_{u1} + i_{v1}$ $i_{wl} = -i_{v1}$
Mode IV	Mode V	Mode VI
$i_{ul} = -i_u - i_{w1}$ $i_{vl} = i_{u1}$ $i_{wl} = i_{w1}$	$i_{ul} = -i_{w1}$ $i_{vl} = -i_v$ $i_{wl} = i_{v1} + i_{w1}$	$i_{ul} = i_{u1}$ $i_{vl} = -i_{u1} + i_{v1}$ $i_{wl} = i_v$

Table 2 shows the line current for each switching mode using the parameters of the cutset equation. The current characteristics in the time domain can be calculated using the relationship between the phase current obtained from the state equation and the cutset equation, and the generated torque of the motor can be calculated using this current.

2.4 Flowchart for numerical analysis

The winding of the stator can be either Δ or Y connection, so in this study, a brushless DC motor was modeled mathematically for the case of Δ connection. As the first step in the analysis, parameters such as voltage, current and inductance are set and the firing angle to be analyzed is

determined. Second, a cut set equation is established and a system matrix for analysis is constructed. Third, the differential equation is solved using the Runge-Kutta method, and then the phase current and the line current are obtained. Also, the torque is calculated using the back electromotive force and current. The system of differential equations is repeatedly analyzed until a steady state is reached by adjusting the time (dt) of the differential equation. Harmonic analysis is performed on the results obtained through Fourier series analysis. Finally, if this whole process is repeatedly performed by changing the firing angle, current and torque characteristics according to the firing angle change can be obtained, and the harmonic spectrum of this result can be analyzed. Figure 5 shows the flowchart of the numerical analysis for Δ connection BLDCM.

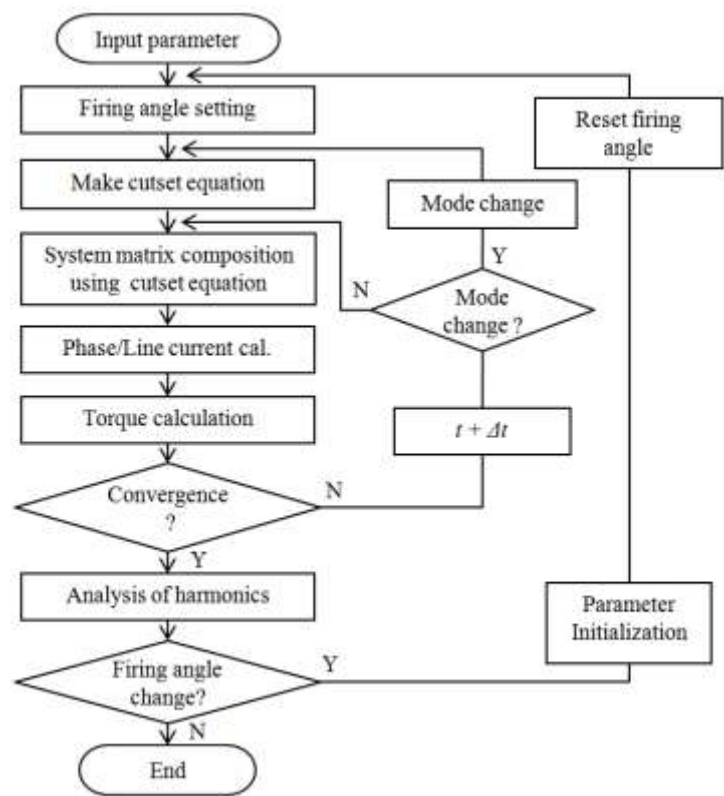


Figure 5. Flowchart for simulation

3. Numerical Results

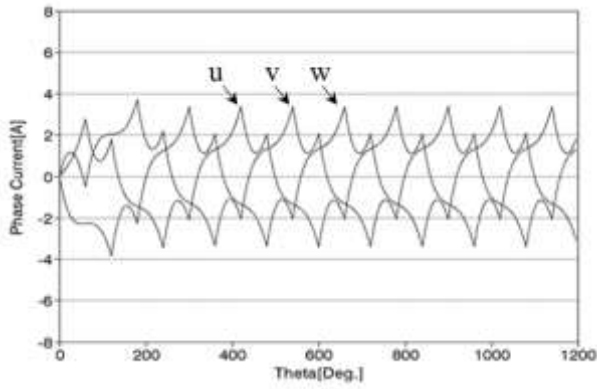
The steady state characteristics of BLDCM were analyzed through computer simulation for each operation mode. Here, the rotor speed is constant and the back electromotive force is a sine wave. In this study, the firing angle of BLDCM was set to 0[Deg.] and the firing angle of maximum torque generation was set to 30[Deg.]. As analysis results, voltage, current, harmonic spectrum and torque waveforms were analyzed. Table 3 shows the circuit constants and rated specifications of the motors used in the analysis.

Table 3: Simulation specification

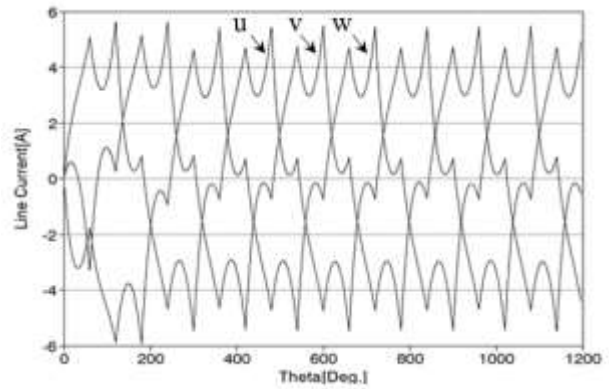
Spec.	Value	Spec.	Value
No. of phase	3	No. of poles	2
Rated voltage	125 [V]	Rated current	3.3[A]
Rated speed	2,500 [rpm]	Rated torque	7.25[kg-cm]
Self-inductance	16 [mH]	Mutual-Inductance	4.8 [mH]
Emf constant	0.021[v/rpm]	Resistance per phase	3.61 [Ω]

Figure 6 shows the phase current and line current when the BLDCM is Δ -connected and the firing angle is 0[Deg.]. As the current waveform enters the steady state, it can be seen that the three phases are balanced and the magnitude of the

line current is slightly larger than the phase current. Figure 7 shows the generated torque waveform, which reached the steady state through the transient state. The torque is pulsating with a certain period constant in a steady state.



a) Phase current



b) Line current

**Figure 6. Current waveform (Δ connection, firing angle = 0)
angle = 0)**

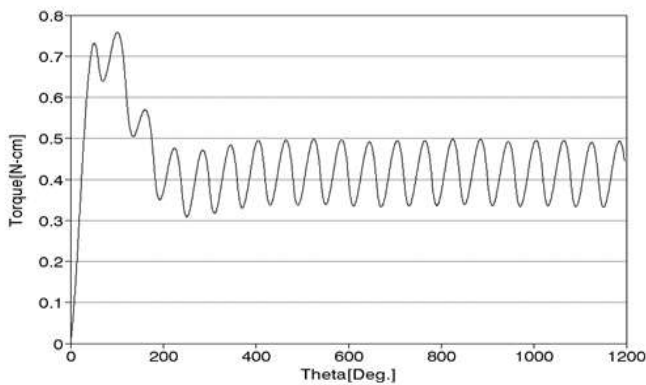
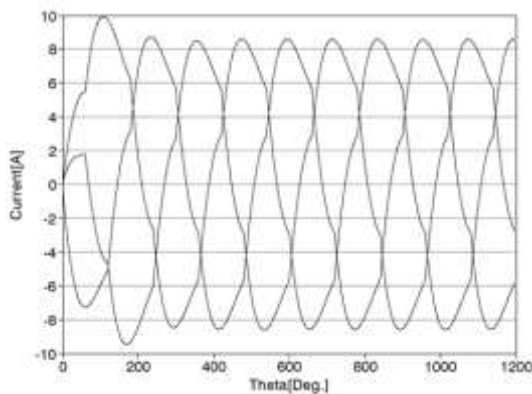
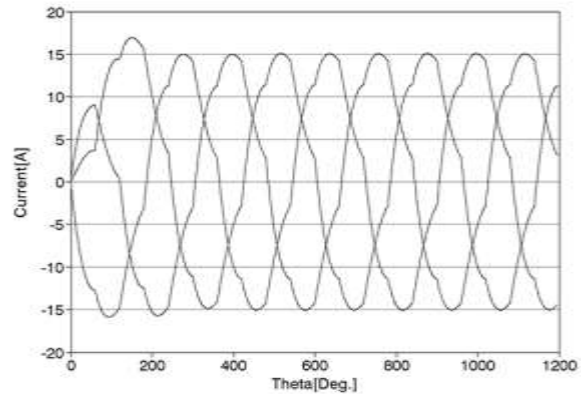


Figure 7. Torque characteristics (Δ connection, firing

Fig. 8 shows the analysis result of phase current and line current in case of delta connection and firing angle is 30 [Deg.]. The results of the current analysis show that two types of current are larger than when the firing angle is 0. Figure 9 shows the torque generated in case of firing angle of 30 [Deg.], which is also much larger than that of firing angle of 0 [Deg.]. The period of the torque waveform appears constant even when the firing angle is changed.



a) Phase current



b) Line current

Figure 8. Current waveform (Δ connection, firing angle = 30)

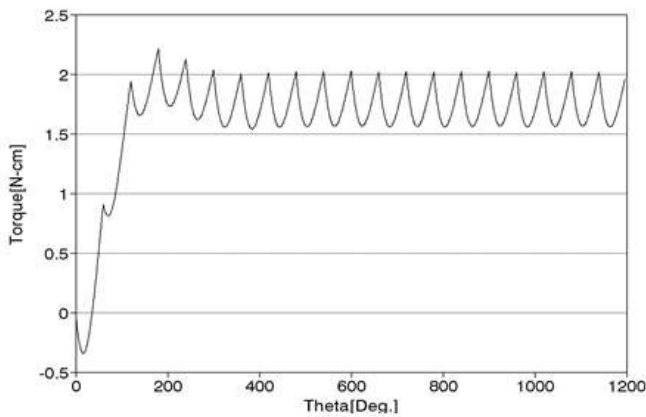


Figure 9. Torque characteristics (Δ connection, firing angle = 30)

Figure 10 shows the results of characteristic analysis while changing the firing angle from 0 to 40 [Deg.]. The phase current, line current and torque of the delta connection are shown, and when the firing angle is 30 [Deg.], the current and torque are the largest.

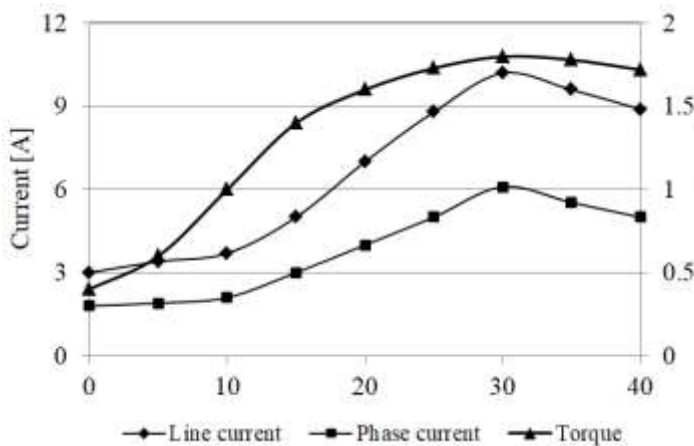


Figure 10. Operating characteristics according to firing angle (Δ connection)

4. Conclusion

When the BLDCM, whose back electromotive force is a sinusoidal wave, is driven by a square wave voltage by a voltage source inverter, the change characteristics of the current component and the generated torque according to the phase angle control of the motor are analyzed. Also, when the firing angle, which is the phase angle between the applied voltage and the counter electromotive force, was adjusted to 0° and 30°, which generates the maximum torque, the winding current, line current, RMS values of current and torque characteristics were analyzed. As a result of simulation, it can be seen that it can be a good reference material for the application and control of BLDCM by analyzing and comparing the change characteristics of the current characteristics and the generated torque according to the phase angle control.

5. Acknowledgment

This paper was supported by Joongbu University Research & Development Fund, in 2021.

6. References

1. Mc Cleer PJ, Bailey JM, Lawler JS, Banerjee B. Five phase trapezoidal back EMF PM synchronous machines and drives. In European Conference on Power Electronics and Applications. 1992;4:128-128.
2. Yedamale P. Brushless DC (BLDC) motor fundamentals. Microchip Technology Inc. 2003 Jul 28;20(1):3-15.
3. Lin YK, Lai YS. Pulse width modulation technique for BLDCM drives to reduce commutation torque ripple without calculation of commutation time. IEEE Transactions on Industry Applications. 2011 May 19;47(4):1786-93.
4. Chen W, Liu Z, Cao Y, Li X, Shi T, Xia C. A position sensorless control strategy for the BLDCM based on a flux-linkage function. IEEE Transactions on Industrial Electronics. 2018 Jun 7;66(4):2570-9.
5. Jiang W, Liao Y, Wang J, Wang P, Xie Y. Improved control of BLDCM considering commutation torque ripple and commutation time in full speed range. IEEE Transactions on Power Electronics. 2017 Jun 20;33(5):4249-60.
6. C. Cui, G. Liu and K. Wang. A Novel Drive Method for High-Speed Brushless DC Motor Operating in a Wide Range. IEEE Transactions on Power Electronics. 2015 Sept;30(9):4998-5008.
7. Wei LZ. A Position Sensorless Control Strategy for BLDCM Based on Line Back-EMF [J]. Transactions of China Electrotechnical Society. 2010;7.
8. F. Naseri, E. Farjah, E. Schaltz, K. Lu, N. Tashakor. Predictive Control of Low-Cost Three-Phase Four-Switch Inverter-Fed Drives for Brushless DC Motor Applications. IEEE Transactions on Circuits and Systems. 2021 Mar;68(3):1308-1318.
9. Shrutika C, Matani S, Chaudhuri S, Gupta A, Gupta S, Singh N. Back-EMF estimation based sensorless control of Brushless DC motor. 2021 1st International Conference on Power Electronics and Energy(IEEE). 2021 Jan 2;1-6.
10. Krishnan R. Permanent magnet synchronous and brushless DC motor drives. CRC press; 2017 Dec 19.
11. Prasad G, Ramya NS, Prasad PV, Das GT. Modelling and Simulation Analysis of the Brushless DC Motor by using MATLAB. International journal of innovative technology and exploring engineering (IJITEE). 2012 Oct;1(5):27-31.
12. Hyun-Seob Cho. Design of Noise Reduction Output Filter for Induction Motor Using H-Bridge Inverter. The journal of next-generation convergence technology association. 2020;4(6):595-600.